Polydopamine as a Biocompatible Multifunctional Nanocarrier for Combined Radioisotope Therapy and Chemotherapy of Cancer

Xiaoyan Zhong, Kai Yang, Zhiliang Dong, Xuan Yi, Yong Wang, Cuicui Ge, Yuliang Zhao, and Zhuang Liu**

Development of biodegradable nanomaterials for drug delivery and cancer theranostics has attracted great attention in recent years. In this work, polydopamine (PDA), a biocompatible polymer, is developed as a promising carrier for loading of both radionuclides and an anticancer drug to realize nuclear-imaging-guided combined radioisotope therapy (RIT) and chemotherapy of cancer in one system. It is found that PDA nanoparticles after modification with poly(ethylene glycol) (PEG) can successfully load several different radionuclides such as ^{99m}Tc and ^{131}I, as well as an anticancer drug doxorubicin (DOX). While labeling PDA-PEG with ^{99m}Tc (^{99m}Tc-PDA-PEG) enables in vivo single photon emission computed tomography imaging, nanoparticles co-loaded with ^{131}I and DOX (^{131}I-PDA-PEG/DOX) can be utilized for combined RIT and chemotherapy, which offers effective cancer treatment efficacy in a remarkably synergistic manner, without rendering significant toxicity to the treated animals. Therefore, this study presents an interesting class of biocompatible nanocarriers, which allow the combination of RIT and chemotherapy, the two extensively applied cancer therapeutic strategies, promising for future clinic translations in cancer treatment.

1. Introduction

Nowadays, cancer as one of leading causes of death remains to be a great challenge to global healthcare.[1,2] Up to date, surgery, radiotherapy, and chemotherapy are still the three major cancer treatment approaches widely used in the clinic.[3–11] However, current chemotherapy and radioisotope therapy (RIT) of cancer both suffer from the nonspecific distribution and low effective tumor uptake of therapeutic agents, severe side effects to normal tissues, as well as the development of multidrug resistance after a certain period of treatment.[12–16] In the past few decades, nanomedicine that employs nanoparticles as drug delivery carriers to improve the pharmacokinetics and bioavailability of therapeutic agents, as well as to realize tumor-targeted drug delivery, has received tremendous attention in both fundamental research and clinical practices.[17–34] Moreover, nanoparticles often could act as multifunctional platforms into which several different types of therapeutic molecules together with imaging agents are loaded, aiming at imaging-guided combination therapy of cancer to achieve the optimized therapeutic outcomes.

Currently, there have been numerous types of nanomaterials, including various inorganic and organic nanoparticles, being explored as drug delivery systems. Among those nanocarrier systems, polydopamine (PDA) has recently received substantial interests owing to its excellent biocompatibility as well as easy surface modification.[35–37] In a number of latest studies, PDA has been utilized as a universal surface modification agent for functionalization of nanoparticles, a light-absorbing agent for photothermal therapy, as well as a novel platform for biosensing and bioimaging.[35,38–42] However, the use of PDA alone as a biocompatible nanocarrier for the delivery of both radionuclides and anticancer drug to realize combined RIT and chemotherapy (radio-chemotherapy) in one nanoparticle system has not yet been demonstrated to our best knowledge.

In this work, we develop PDA nanoparticles as multifunctional nanocarriers to load with two types of radionuclides and an anticancer drug, for imaging-guided combined internal RIT and chemotherapy in cancer treatment (**Figure 1**). PDA

X. Zhong, Prof. K. Yang, X. Yi, Dr. Y. Wang, Prof. C. C. Ge
School of Radiation Medicine and Protection and School for Radiological and Interdisciplinary Sciences (RAD-X)
Collaborative Innovation Center of Radiation Medicine of Jiangsu Higher Education Institutions
Medical College of Soochow University
Suzhou, Jiangsu 215123, P. R. China
E-mail: kyang@suda.edu.cn

Z. Dong, Prof. Z. Liu
Institute of Functional Nano & Soft Materials (FUNSOM) and Collaborative Innovation Center of Suzhou Nano Science and Technology Soochow University
Suzhou, Jiangsu 215123, P. R. China
E-mail: zliu@suda.edu.cn

Prof. Y. Zhao
CAS Key Laboratory for Biomedical Effects of Nanomaterials and Nanosafety
Institute of High Energy Physics
Chinese Academy of Sciences
Beijing 100049, P. R. China

DOI: 10.1002/adfm.201503587

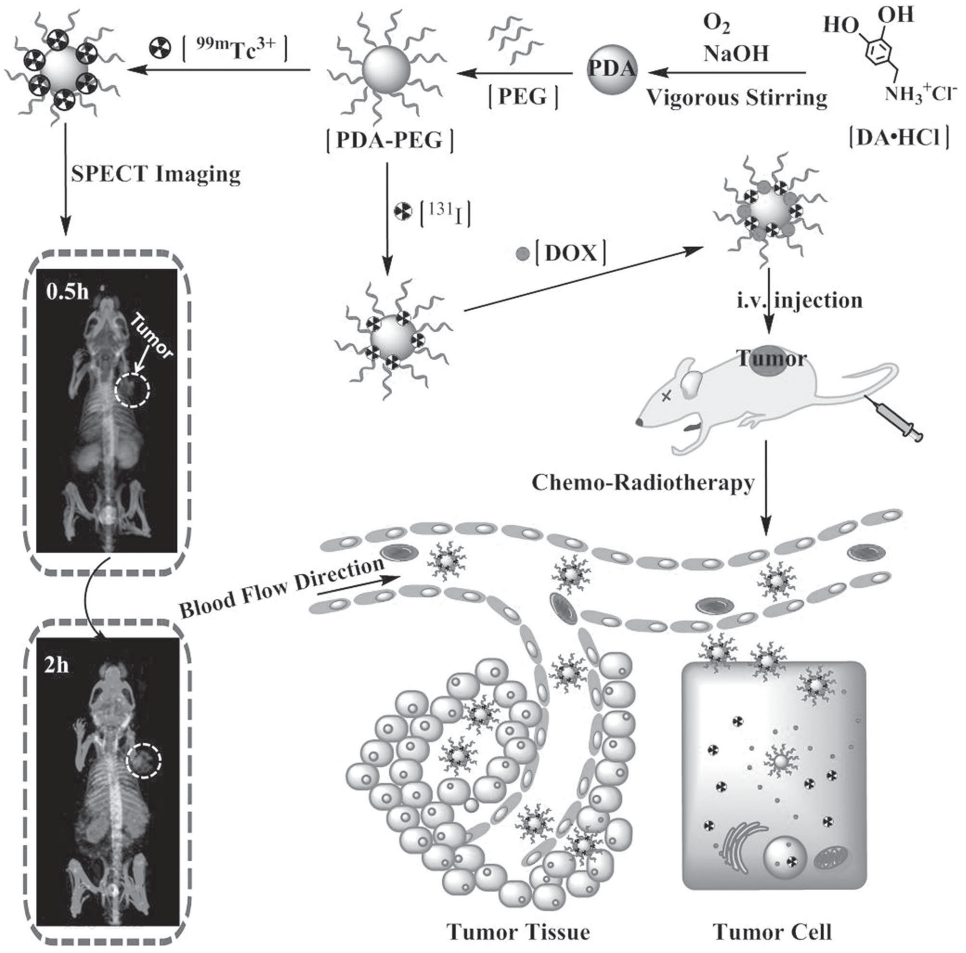

Figure 1. Schematic to show ^{99m}Tc or ^{131}I labeled PEGylated PDA nanoparticles with DOX loading for SPECT imaging and combined radio–chemotherapy.

nanoparticles are synthesized from dopamine hydrochloride by a simple aqueous phase method and functionalized with polyethylene glycol (PEG) to improve their physiological stability. While ^{99m}Tc, a radionuclide commonly used for single photon emission computed tomography (SPECT) imaging, is introduced to label PDA-PEG nanoparticles upon simple mixing PDA-PEG with chemically reduced ^{99m}Tc, ^{131}I which has been widely applied in RIT can be conjugated on PDA-PEG nanoparticles via the standard chloramine T oxidation method. In the meanwhile, doxorubicin (DOX), a chemotherapeutic drug, also can be loaded on PDA-PEG nanoparticles with high efficiency. SPECT imaging of tumor-bearing mice intravenously (i.v.) injected with ^{99m}Tc-labeled PDA-PEG nanoparticles reveals efficient tumor uptake of nanoparticles. In vivo combined RIT and chemotherapy is further carried out with ^{131}I-labeled/DOX-loaded PDA-PEG (^{131}I-PDA-PEG/DOX), achieving rather effective cancer treatment efficacy in a mouse tumor model with a superior treatment outcome realized compared to the respective monotherapies. Furthermore, it is found that ^{131}I-PDA-PEG/DOX induces no obvious toxicity to treated mice at the therapy dose within 80 d. Our work demonstrates that PEGylated PDA nanoparticle can act as excellent biocompatible multifunctional nanocarrier to load various distinctive types of therapeutic and imaging molecules, and may become a great platform to realize imaging-guided combination cancer treatment.

2. Results and Discussion

In our work, PDA was synthesized from dopamine hydrochloride via a simple and green method according to the previous protocol.[43] Dopamine hydrochloride was polymerized at pH 9.0 by adding sodium hydroxide under vigorous stirring in the presence of oxygen at 50 °C. After 5 h of polymerization, the solution color changed into dark brown, indicating PDA formation. As revealed by scanning electron microscope (SEM), PDA nanoparticles showed uniform spherical morphology, while the hydrodynamic size of PDA was measured to be around ≈120 nm by dynamic light scattering (DLS) (**Figure 2**a). Although as-made PDA nanoparticles were well-dispersed in water, their colloidal stability in physiological solutions containing salts was not good. Therefore, amine-terminated PEG was introduced to functionalize PDA nanoparticles under pH 12.0 via the Michael addition and/or Schiff base reaction.[35,44,45] The obtained PDA-PEG nanoparticles exhibited great stability in various physiological solutions (Figure 2c). Because of the PEG coating, the average hydrodynamic diameter of PEG-functionalized PDA

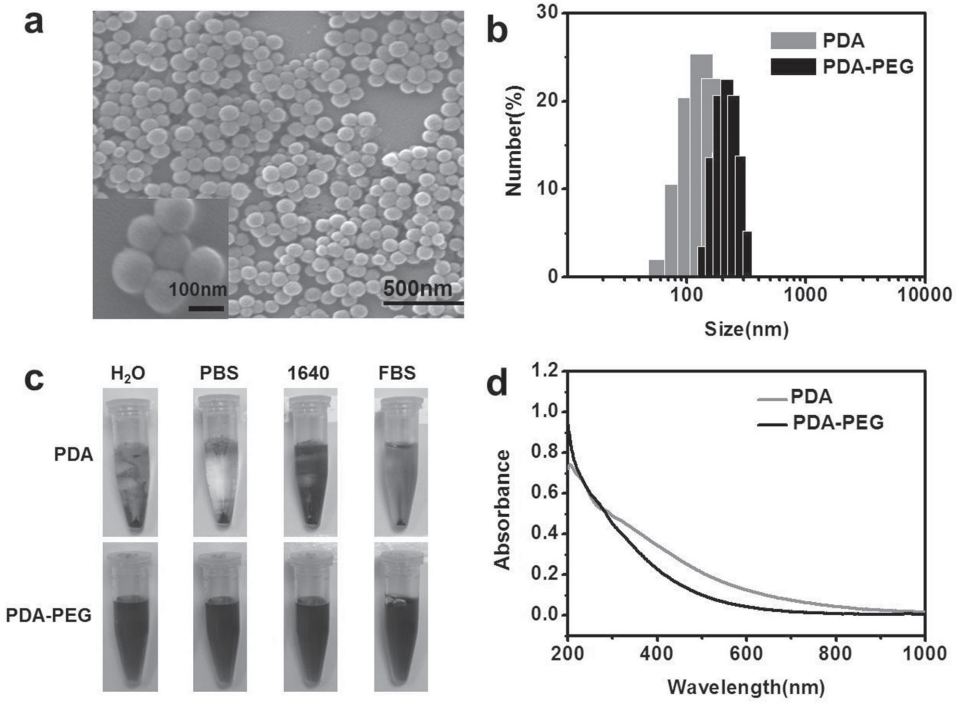

Figure 2. Preparation and characterization of PDA nanoparticles. a) SEM images of PDA nanoparticles. b) Size distributions of PDA and PDA-PEG in water measured with DLS. c) Photographs of PDA and PDA-PEG in different solutions. d) UV–vis–NIR spectra of PDA before and after PEGylation.

became larger (≈200 nm) (Figure 2b). After PEGylation, the zeta potential of nanoparticles also showed a slight increase (Supporting Information). Similar to as-made PDA, PDA-PEG solution exhibited broad band absorption from ultraviolet to near-infrared ranges (Figure 2d).

We then would like to test the ability of PDA-PEG to load various types of therapeutic and imaging agents (**Figure 3**a). DOX, a commonly used anticancer drug with an aromatic molecular structure, could be loaded on the surface of sp^2-bonded carbon nanostructures or conjugated polymers via hydrophobic interaction and π–π stacking.[17,36,46–53] We thus wondered whether similar behavior could be observed for PDA, which also contains conjugated polymeric structures. For DOX loading, PEGylated PDA solution (1 mg mL^{-1}) was mixed with different amounts of DOX at pH 7.4 for 6 h. Unbound DOX was completely removed by centrifugal filtration. The obtained DOX loaded PDA-PEG nanoparticles (PDA-PEG/DOX) were readily dispersed in water, forming a clear solution with reddish color (Supporting Information, Figure S2). The loading of DOX on PDA-PEG nanoparticles, which resulted in the increase of nanoparticle zeta potential, was determined from the characteristic UV–vis absorbance peak of DOX at 490 nm superimposed on the PDA-PEG absorption spectrum (Figure 3b and Supporting Information, Figure S1). The DOX loading ratios (DOX:PDA, w/w) increased with increasing amounts of added DOX (Figure 3c). Considering the fact that too much DOX loading would affect the stability of nanoparticles, PDA-PEG/DOX with a moderate DOX loading of ≈66% (DOX:PDA, w/w) achieved at a feeding DOX:PDA weight ratio of 1:1 was used for our followed experiments. As expected, accelerated drug release was observed for PDA-PEG/DOX at a lower pH, owing to the protonation of amino group in the DOX molecule that gives DOX a positive charge and thus the enhanced hydrophilicity to trigger DOX release (Supporting Information, Figure S3).[54]

In order to realize imaging guided RIT, radionuclides ^{99m}Tc and ^{131}I, were introduced to label PDA-PEG separately. While ^{99m}Tc is a gamma-ray emitter widely applied for SPECT imaging, ^{131}I that emits strong beta particles is particularly useful in RIT of cancer. Owing to the existence of various functional groups such as catechol, amine, and imine on the surface of nanoparticles, PDA could be used as an excellent nanocarrier to bind metal ion via chelation reaction.[55,56] For ^{99m}Tc labeling, a $^{99m}TcO_4^-$ solution (≈1 mCi) was added into the PDA-PEG solution in the presence of a reducing agent, stannous chloride (200 µL, 5 mg mL^{-1}), under magnetic stirring at room temperature. After 1 h of reaction, the reduced $^{99m}Tc^{3+}$ was completely chelated by the various functional groups on PDA, obtaining ^{99m}Tc labeled PDA-PEG (^{99m}Tc-PDA-PEG) with excellent radio-stability in phosphate buffered saline (PBS) and serum solutions at 37 °C (Figure 3a,d). The labeling yield was determined to be as high as ≈99%. On the other hand, ^{131}I was introduced to label PDA-PEG in the presence of chloramines-T, which may oxidize I^- ions into I atoms to attack benzene rings in polymerized dopamine via electrophilic substitution reaction (Figure 3a). The ^{131}I labeled PDA-PEG exhibited a high radiolabeling yield at 70%, as well as great radiolabeling stability in PBS and serum at 37 °C (Figure 3a,e). Therefore, radionuclide ^{99m}Tc and ^{131}I could be introduced to label PDA-PEG via different mechanisms both with high efficiencies and stabilities (Figure 3a).

Before studying in vivo combined radio-chemotherapy therapeutic performance of ^{131}I-PDA-PEG/DOX, we first tested its

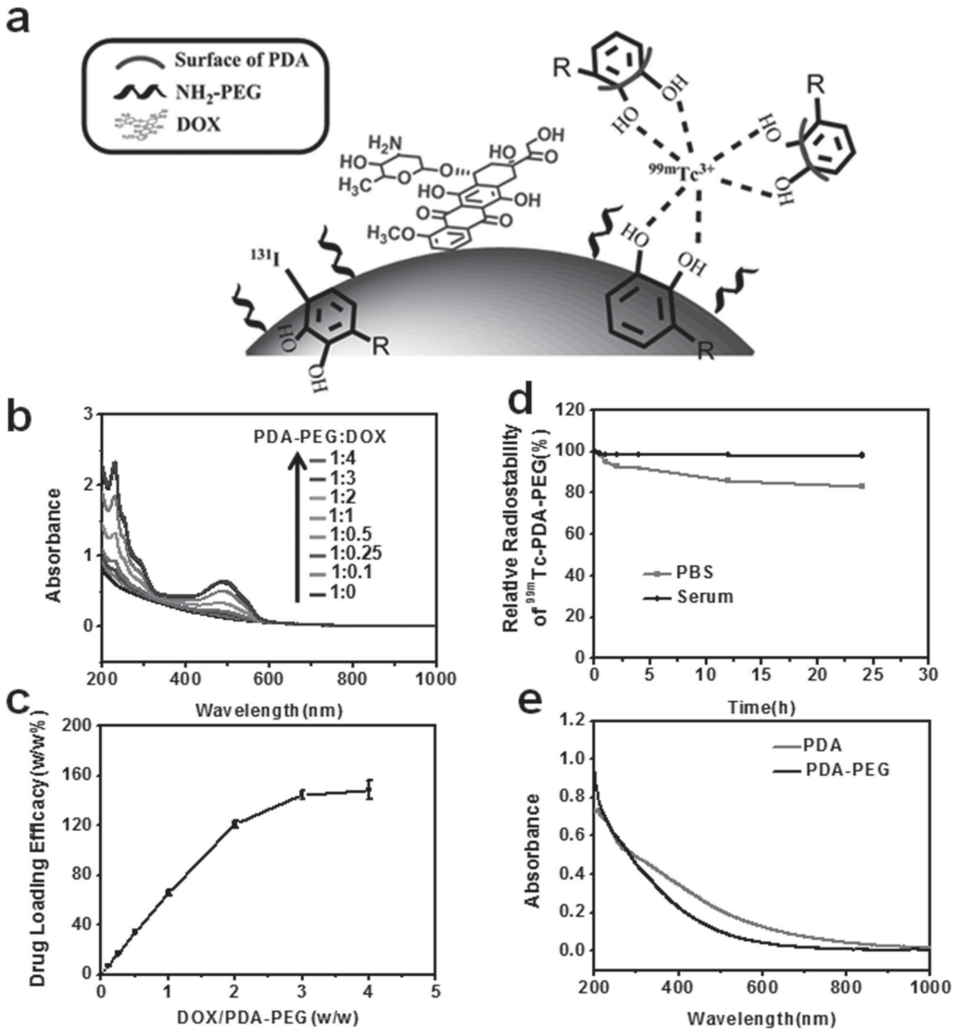

Figure 3. Radiolabeling and drug loading on PDA-PEG. a) Schematic of radiolabeing and drug loading on PDA-PEG via different mechanisms. b) UV–vis–NIR absorbance spectra of PDA-PEG and PDA-PEG/DOX obtained at different PDA:DOX feeding ratios. c) Quantification of DOX loading at different feeding amounts of DOX. d) The radiostability of ^{99m}Tc-PDA-PEG and e) ^{131}I-PDA-PEG after incubation in PBS or serum.

potential toxicity to cancer cells using the cell counting kit-8 (CCK-8) assay. Murine breast cancer 4T1 cells were incubated with PDA-PEG, free ^{131}I, free DOX, ^{131}I-PDA-PEG, PDA-PEG-DOX, and ^{131}I-PDA-PEG-DOX at different concentrations for 24 h. It was found that PDA-PEG induced no obvious toxicity to cells even at an ultrahigh concentration of 1000 mg mL^{-1}, suggesting the great biocompatibility of PEGylated PDA nanoparticles (**Figure 4**a). We next compared the potential toxicity of free ^{131}I and ^{131}I labeled PDA-PEG to 4T1 cells. Interestingly, ^{131}I-PDA-PEG exhibited higher toxicity than free ^{131}I under the same doses of radioactivity (Figure 4b), owing to the greatly enhanced cellular uptake of ^{131}I delivered by PDA-PEG (data not shown), which has been demonstrated in our previous work with another type of nanoparticle system.[21] In addition, we also investigated the potential toxicity of free DOX and PDA-PEG/DOX to cells. It was found that DOX loaded PDA-PEG exhibited similar toxicity to cells compared with free DOX at the same DOX concentrations (Figure 4c). For the combination of RIT and chemotherapy, 4T1 cells were incubated with ^{131}I-PDA-PEG/DOX, ^{131}I-PDA-PEG, and PDA-PEG/DOX at the different concentrations for 24 h. The combined RIT + chemotherapy treatment with ^{131}I-PDA-PEG/DOX was found to be highly effective in destructing cancer cells, obviously superior to single treatment by either ^{131}I-PDA-PEG or PDA-PEG/DOX (Figure 4d). Therefore, ^{131}I and DOX could be co-transported into cells by PEGylated PDA nanoparticles to achieve the combination of RIT and chemotherapy for rather effective cancer cell killing.

With its strong gamma-ray emission and short half-life (6.02 h), ^{99m}Tc is a widely used radioactive tracer in the clinic for SPECT imaging. In our work, ^{99m}Tc-PDA-PEG (800 mCi per mouse, 10 mg kg^{-1} of PDA-PEG) was intravenously (i.v.) injected into 4T1 tumor-bearing mice, which were then imaged by the U-SPECT system (MILabs, Utrecht, the Netherlands) at different time points post injection (p.i.). Obvious tumor uptake of ^{99m}Tc-PDA-PEG showed up after 2 h p.i. (**Figure 5**a). The tumors of mice treated with ^{99m}Tc-PDA-PEG were collected after imaging scanning at different time points for quantitative

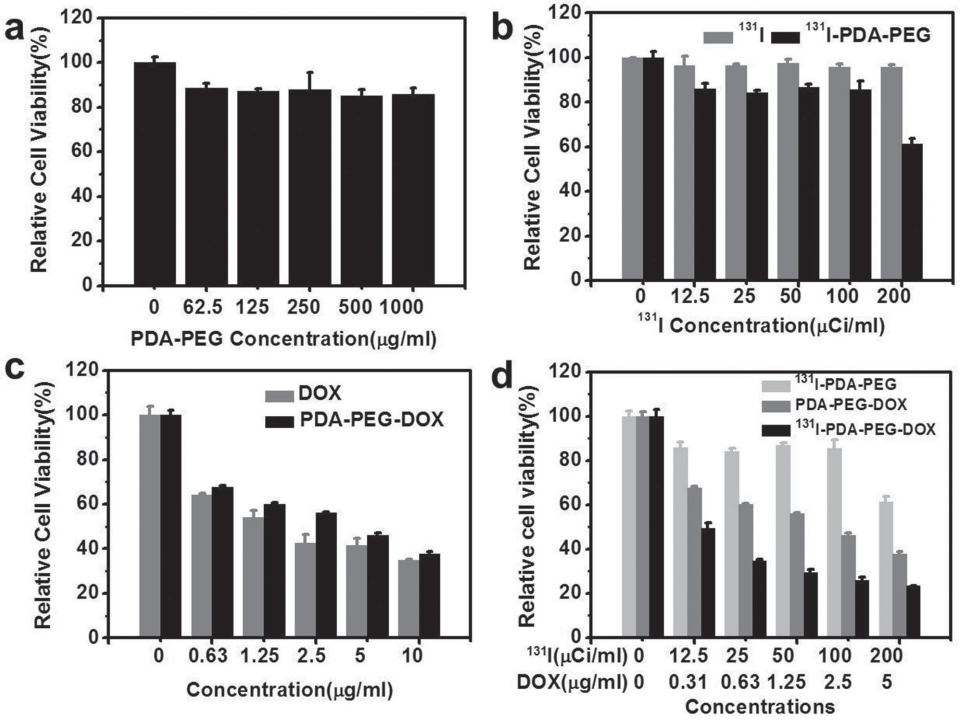

Figure 4. In vitro chemotherapy and radioisotope therapy experiments. a) The relative viabilities of 4T1 cells after being incubated with different concentrations of PDA-PEG for 24 h. b) The relative viabilities of 4T1 cells after being incubated with different concentrations of free ^{131}I and ^{131}I-PDA-PEG for 24 h. c) The relative viabilities of 4T1 cells after being incubated with different concentrations of free DOX and PDA-PEG/DOX for 24 h. d) The relative viabilities of 4T1 cells after being incubated with different concentrations of ^{131}I-PDA-PEG, PDA-PEG/DOX, and ^{131}I-PDA-PEG/DOX for 24 h. These results showed that ^{131}I-PDA-PEG/DOX exhibited higher toxicity than ^{131}I-PDA-PEG or PDA-PEG/DOX treatment alone.

measurement by a gamma counter. It was found that ^{99m}Tc-PDA-PEG could passively accumulate in the tumor, likely via the enhanced permeability and retention (EPR) effect (Supporting Information, Figure S4). In addition, substantial accumulation of radioactivity was also noticed in the liver, kidney, as well as bladder, the latter of which indicated the possible degradation of PDA and/or partially detachment of ^{99m}Tc labeling from PDA-PEG nanoparticles in vivo.

The short half-life of ^{99m}Tc makes it not ideal for in vivo tracking over a relatively long period of time. We thus used ^{131}I with a half-life of 8 d to track the blood circulation and biodistribution of PEGylated PDA nanoparticles, which were first labeled with ^{131}I and then loaded with DOX. After i.v. injection of ^{131}I-PDA-PEG/DOX (10 mg kg^{-1} of PDA-PEG, 20 mCi of ^{131}I) into Balb/c mice with thyroid blocked with preinjection of cold NaI, blood was drawn from the right side of orbital venous plexus of mice at different time points p.i. and measured by a gamma counter to determine the radioactivity of blood samples. The blood circulation curve showed that the pharmacokinetics of the ^{131}I-PDA-PEG/DOX followed a two-compartment model. The first and second phase blood circulation half-lives were measured to be 0.77 ± 0.39 h and 11.58 ± 4.43 h, respectively (Figure 5b), which appeared to be rather long-time among various drug delivery carriers. For the biodistribution of ^{131}I-PDA-PEG/DOX, we sacrificed the mice at 24 h p.i. and collected their tumors and major organs for radioactivity measurement by the gamma counter. It was found that ^{131}I-PDA-PEG/DOX exhibited substantial uptake in tumor, in which the radioactivity level ranked the 2nd among various major organs (about two-thirds of the liver uptake) (Figure 5c). The retention of radioactivity in reticuloendothelial systems (RES) became relatively low at 24 h p.i., likely owing to the gradual degradation of PDA and the clearance of radioactivity over time.

Encouraged by the imaging and biodistribution data, we then used ^{131}I-PDA-PEG/DOX as a therapeutic agent for in vivo combined RIT and chemotherapy. Balb/c mice bearing 4T1 tumors were randomly divided into six groups with five mice per group including (1) PBS, (2) PDA-PEG, (3) PDA-PEG/DOX, (4) ^{131}I-PDA-PEG, (5) the mixture of free DOX and ^{131}I, and (6) ^{131}I-PDA-PEG/DOX. The doses of PDA-PEG, DOX, and ^{131}I were 10 mg kg^{-1}, 5 mg kg^{-1}, and 200 mCi per mouse, respectively (see detailed information in the Experimental Section). The above treatments were given by i.v. injection into mice bearing 4T1 tumors every 4 d for four times. The tumor volumes were monitored by a caliper every other day (**Figure 6**a). Compared to control mice treated with PBS or free PDA-PEG, tumors on mice after chemotherapy with PDA-PEG/DOX or RIT with ^{131}I-PDA-PEG showed only partially reduced growth speed. In marked contrast, mice after treatment with ^{131}I-PDA-PEG/DOX showed greatly inhibited tumor growth. The tumor sizes were well controlled without further growth after four rounds of combined chemotherapy + RIT with ^{131}I-PDA-PEG/DOX. Notably, the same doses of combination therapy with free DOX and free ^{131}I resulted in unsatisfactory therapeutic effect, likely owing to the poor pharmacokinetics profiles and low tumor retention of those small molecule agents after i.v. injection. Importantly,

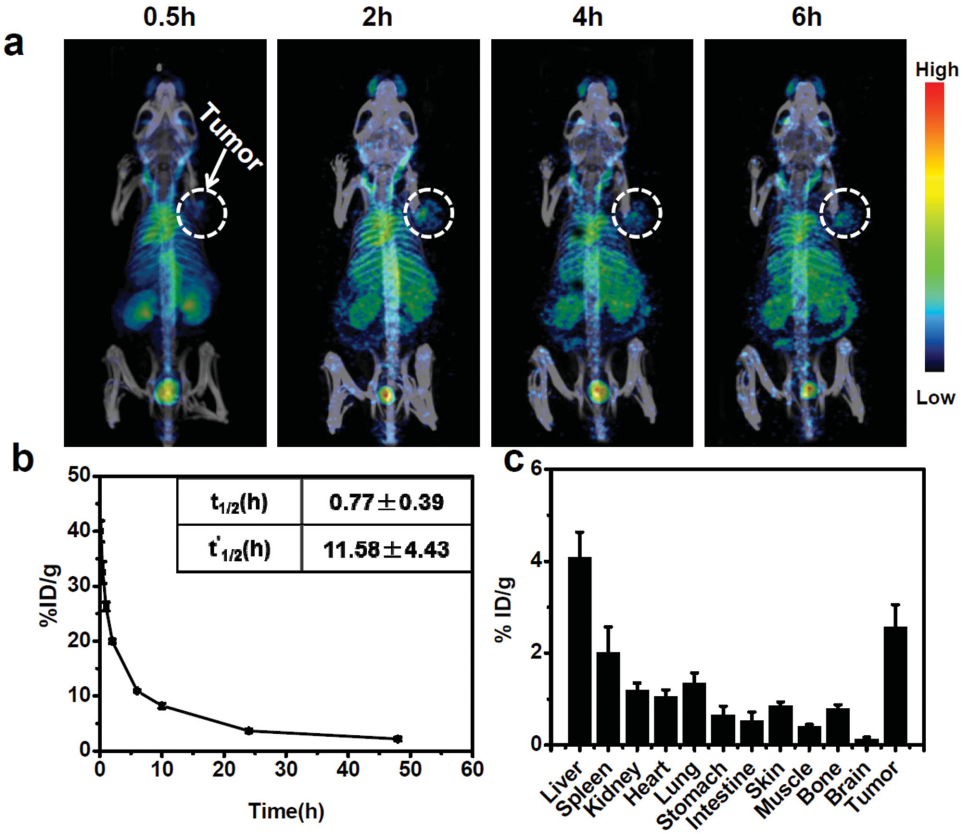

Figure 5. In vivo behavior of radioisotope labeled PDA-PEG. a) SPECT imaging of 4T1-tumor-bearing mice after i.v. injection with ^{99m}Tc-PDA-PEG taken at the different time points post injection. b) The blood circulation of ^{131}I-PDA-PEG/DOX. c) The biodistribution of ^{131}I-PDA-PEG/DOX measured at 24 h postinjection.

compared to mice in those control groups which showed short survival time (two to three weeks), mice in the ^{131}I-PDA-PEG/DOX treated group exhibited greatly prolonged survival without a single death within four weeks after treatment (Figure 6b).

To further investigate the tumor damage degree after different treatments, we performed Hematoxylin & Eosin (H&E) staining to examine tumors from mice that received different treatments at 16 d p.i. While partial tumor damages were

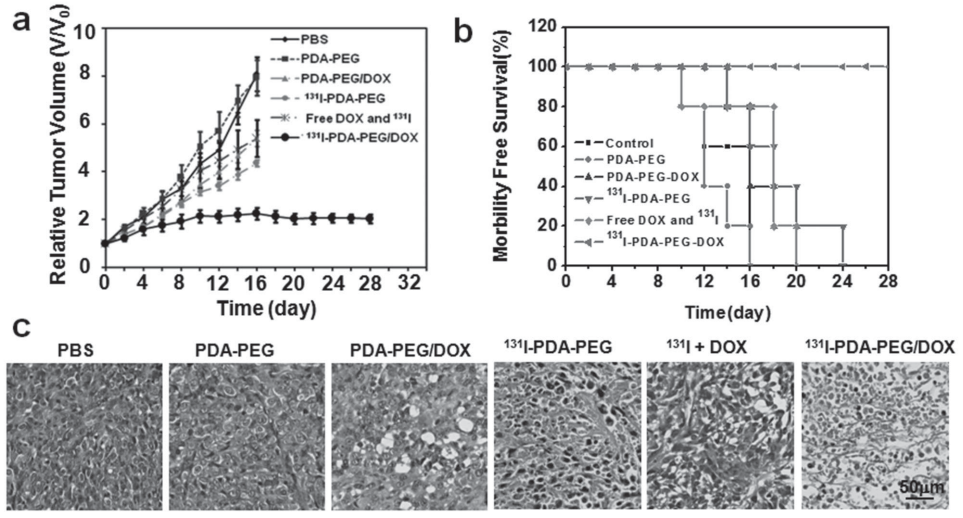

Figure 6. In vivo combination therapy based on ^{131}I-PDA-PEG/DOX. a) Tumor growth curves of mice with different treatments given at day 0, 4, 8, and 12. Five mice were used for each group. Doses for each injection: 5 mg kg^{-1} of DOX, 100 mCi of ^{131}I. The tumor volumes were normalized to their initial sizes. b) The survival curves of mice after various treatments during the period of observation lasted for 28 d. c) Micrographs of H&E stained tumor slices from mice with different treatments collected 16 d after the treatment was finished.

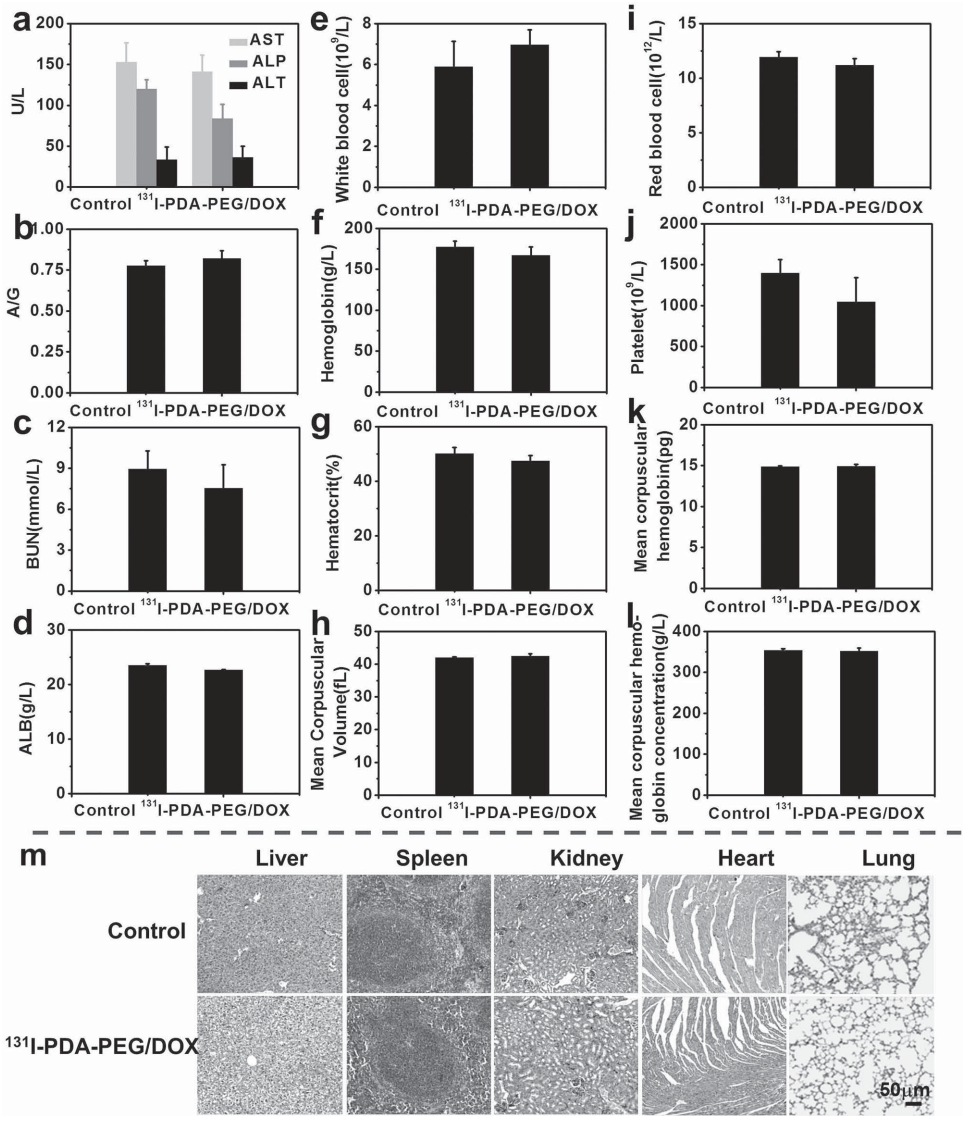

Figure 7. In vivo toxicology evaluation of ^{131}I-PDA-PEG/DOX. a–l) Healthy female Balb/c mice were i.v. injected with four doses of ^{131}I-PDA-PEG/DOX (5 mg kg^{-1} of DOX, 100 mCi of ^{131}I) at day 0, 4, 8, and 12, and sacrificed at day 80 for blood analysis including serum biochemistry (a–d) and hematology measurements (e–l). Age-matched untreated mice were used as the control. m) The H&E staining of major organs. There was no obvious morphological changes, compared with the control group.

noted for mice after treatment with ^{131}I-PDA-PEG, PDA-PEG/DOX, as well as the mixture of free DOX and free ^{131}I, tumors from mice receiving combination therapy with ^{131}I-PDA-PEG/DOX showed the highest level of tumor cell damage, as indicated by the complete loss of cell morphology and structures in this group (Figure 6c). Although the detailed synergistic mechanism in such combination therapy remains to be further discovered, it is obvious that combining chemotherapy with RIT using PEGylated PDA nanoparticles as the nanocarrier offers remarkable advantages in cancer treatment with greatly enhanced therapeutic efficacy.

Toxic side effects to normal tissues have been the main problem of cancer chemotherapy and internal RIT. In this work, we also investigated the potential toxicity of ^{131}I-PDA-PEG/DOX to treated mice. Healthy Balb/c mice (n = 5) were i.v. injected with ^{131}I-PDA-PEG/DOX at the same therapeutic dose every four days for four times. Their blood was collected for blood biochemistry and complete blood panel assay at 80 d p.i. Other five age-matched mice were used as control. The liver and kidney function markers and the ratio of albumin and globulin (A/G) were measured to be normal compared with the control group (**Figure 7**a–d). For blood routine examination, various parameters were measured and fell well into the normal reference ranges compared with the control group, indicating that ^{131}I-PDA-PEG/DOX induced no obvious toxicity to treated mice within 80 d (Figure 7e–l). Meanwhile, major organs from mice treated with or without ^{131}I-PDA-PEG-DOX were also collected for H&E staining and histological examination. No significant organ damage was observed in mice treated with ^{131}I-PDA-PEG/DOX (Figure 7m). Therefore, the combination treatment with ^{131}I-PDA-PEG/DOX showed no significant long-term toxicity to the treated animals.

3. Conclusion

In summary, our study presents a new type of multifunctional nanocarrier based on polydopamine with great biocompatibility for combination cancer treatment. In this system, PDA formed by spontaneous air oxidization of dopamine is PEGylated by simply mixing amine-terminated PEG with PDA nanoparticles under a basic pH condition. The obtained PDA-PEG nanoparticles showed great physiological stability and long blood circulation time. Utilizing the unique chemical structure of PDA, two types of radioisotopes, ^{99m}Tc and ^{131}I, may be attached to PDA nanoparticles with high radiolabeling yields and stabilities. In the meanwhile, it is found that an aromatic chemotherapy drug, DOX, can be physically adsorbed on PDA-PEG nanoparticles with high drug loading efficiency, likely via π–π stacking and hydrophobic interaction. While ^{99m}Tc labeling enables SPECT imaging to real-time track the distribution of nanoparticles in mice, conjugation of ^{131}I and loading of DOX make the obtained ^{131}I-PDA-PEG/DOX nanoparticles a great nanodrug for combined radio-chemotherapy, which offers excellent synergistic therapeutic outcomes to treat tumors on mice upon systemic administration. Considering the great biocompatibility of PDA and the no obvious toxic side effect observed for mice after combination therapy with ^{131}I-PDA-PEG/DOX, such drug-loaded, radioisotope-labeled PDA nanoparticles may have great potential as a safe and effective nanodrug promising for combination therapy of cancer. Moreover, the unique radiolabeling and molecular loading behaviors of PDA discovered in this work may be extended to the other types of radioisotopes (for imaging and therapy) or molecules (for imaging, therapy, and targeting) of interests, to develop novel PDA-based nanoagents with interesting functions and properties useful in biomedicine.

4. Experimental Section

Synthesis and Functionalization of Polydopamine (PDA) Nanoparticles: PDA nanoparticles were synthesized by a facile approach according to the previous protocols.[43] In brief, 180 mg of dopamine hydrochloride (Aldrich Chemical) was dissolved in 90 mL of deionized water, and then added with 760 µL of sodium hydroxide (NaOH, 0.2 mol L^{-1}) under magnetic staining at 50 °C. The color of the solution changed from pale yellow to dark brown gradually. After polymerization for 5 h, as-prepared PDA nanoparticles were collected by centrifugation at 14 000 rpm and washed with deionized (DI) water until no color in the supernatant. The obtained PDA nanoparticles were covalently functionalized with amine-terminated PEG (mPEG-NH_2, 5kDa). 100 mg of mPEG-NH_2 dissolved in 1 mL of DI water was added dropwisely into 5 mL of PDA solution (2 mg mL^{-1}) at pH 12.0 under sonication for 30 min. The reaction solution was stirred overnight, obtaining PDA-PEG nanoparticles which were purified by filtration through 10 kDa molecular weight cut-off (MWCO) Amicon filters to remove excess PEG and stored under 4 °C for future experiments.

DOX Loading and Release: DOX (Beijing Huafeng United Technology Co, Ltd.) loading onto PDA-PEG was conducted by mixing 1 mL of PDA-PEG solution (1 mg mL^{-1}) with different amounts of DOX (0.1–4 mg) in phosphate buffer (20×10^{-3} M) at pH 8. The mixture was stirred for 6 h in dark. Unbound excess DOX was then removed by centrifuge filtration with 10 kDa MWCO filters and washed with DI water several times. The obtained DOX-loaded nanoparticles were re-suspended in DI water and stored at 4 °C for next experiments. UV–vis–NIR was used to measure the DOX loading efficiency. Fluorescence spectra of free DOX and PDA-PEG-DOX were measured by FluoroMax 4 fluorometer (Horiba). For DOX releasing measurement, PDA-PEG-DOX solutions were dialyzed in PBS at pH 5.0 and 7.4 in dark and kept in a 37 °C water bath. At different time points, DOX released from PDA-PEG-DOX was collected and measured by UV–vis–NIR spectra.

^{131}I Labeling: PDA-PEG was labeled with radionuclide ^{131}I (purchased from Shanghai GMS Pharmaceutical Co., Ltd) through a standard chloramine-T oxidation method. In brief, 180 µCi of ^{131}I and 10 µL of chloramine T (10 mg mL^{-1}) were added into the solution of PAD-PEG (1 mg mL^{-1}, 1 mL). The mixture was then reacted in a pH 7.5 phosphate buffer (50×10^{-3} M) for 10 min at room temperature. Excess ^{131}I was removed by centrifugation filtration through Amicon filters (MWCO = 10 kDa) and washed several times with DI water until no detachable radioactivity in the filtration solution. For the radiolabeling stability assay, 5 mL of the obtained ^{131}I-PDA-PEG (1 mg mL^{-1}) was mixed with 500 mL of PBS or serum at 37 °C in a water bath. Free ^{131}I was removed by centrifuge filtration through Amicon filters (MWCO = 10 kDa) and washed with water for two times. The leftover ^{131}I-PDA-PEG after washing was collected for gamma counting to measure the amount of retained ^{131}I on PDA-PEG nanoparticles. Next, the obtained ^{131}I-PDA-PEG was used to load DOX at the mass ratio 1:1 (^{131}I-PDA-PEG : DOX) for 6 h. Free DOX was removed by centrifugation and washed with water several times. The achieved ^{131}I-PDA-PEG-DOX was used for in vitro and in vivo experiments.

^{99m}Tc Labeled PDA-PEG for SPECT Imaging: Technetium-99m (^{99m}Tc, purchased from Shanghai GMS Pharmaceutical Co., Ltd) with radioactivity of 6 mCi was added into the PDA-PEG solution (5 mL, 0.2 mg mL^{-1}) in the present of 200 µL of stannous chloride ($SnCl_2$, 5 mg mL^{-1} in 0.1 M HCl) and then stirred gently for 1 h at room temperature. The obtained ^{99m}Tc labeled PDA-PEG solution were purified by ultrafiltration to remove free ^{99m}Tc. The radiolabeling yield was determined to ≈99%. For SPECT imaging, mice bearing 4T1 tumors were intravenous injected with ^{99m}Tc-PDA-PEG nanoparticles at 800 mCi per mouse and imaged by in vivo animal SPECT (MILabs, Utrecht, the Netherlands) imaging system at various time points p.i.

Cellular Experiments: 4T1 murine breast cell line was originally obtained from American Type Culture Collection (ATCC) and cultured in RPMI-1640 supplemented with 10% fetal bovine serum (FBS) and 1% penicillin-streptomycin in a humidified atmosphere containing 5% CO_2 at 37 °C. For the in vitro cytotoxicity assay, 4T1 cells were first seeded into 96-well plates at a density of 5000 cells per well overnight, and then incubated with free DOX, ^{131}I, the mixture of DOX and ^{131}I, PDA-PEG, PDA-PEG-DOX, ^{131}I-PDA-PEG, and ^{131}I-PDA-PEG-DOX at various concentrations for 24 h. Cell counting kit-8 (CCK-8) assay was then conducted to determine the relative cell viabilities related to the untreated control.

Blood Circulation and Biodistribution: All animals were acclimated to the animal facility for 7 d prior to experimental procedures. Healthy female Balb/C mice were intravenously injected with ^{131}I-PDA-PEG (20 µCi of ^{131}I corresponding to 10 mg kg^{-1} of PDA-PEG per mouse). Blood circulation was measured by drawing ≈20 µL of blood from one side of orbital venous plexus at various time points post injection (p.i.). The radioactivity in blood samples were measured by a gamma counter (LB211, Berthold Technologies Gmbh & Co.KG). In order to test the tumor uptake of ^{131}I-PDA-PEG, mice bearing 4T1 tumor were injected with the same dose of ^{131}I-PDA-PEG and sacrificed at 24 h p.i. Major organs including liver, spleen, kidney, heart, lung, stomach, intestine, skin, muscle, bone, brain, and tumor were collected, weighed and measured by the gamma counter.

Combination Therapy: To generate the tumor model, 2×10^6 of 4T1 cells suspended in 50 µL of PBS were subcutaneously injected into the right back of each mouse. Upon the tumor volume reached above 0.15 cm^3 (after nearly 7 d inoculation), the mice were randomly divided into six groups with five mice per group and then differently treated with: 1) PBS, 2) PDA-PEG (10 mg kg^{-1}), 3) the mixture of DOX and ^{131}I (5 mg kg^{-1} of DOX, 200 mCi of ^{131}I), 4) PDA-PEG-DOX (5 mg kg^{-1} of DOX), 5) ^{131}I-PDA-PEG (200 mCi of ^{131}I), and 6) ^{131}I-PDA-PEG-DOX (5 mg kg^{-1} of DOX, 100 mCi of ^{131}I). The above agents were i.v. injected

into mice bearing 4T1 tumor modal every 4 d at day 0, 4, 8, and 12. The tumor volumes were monitored by a caliper every the other day, and calculated according to the following formula: Volume (cm^3) = length (cm) × width^2 (cm^2)/2.

Blood Chemistry Analysis and Histology Examinations: Healthy female Balb/c mice with and without i.v injection of ^{131}I-PDA-PEG-DOX (n = 5 per group) at a dose of 10 mg kg^{-1} of PDA-PEG (corresponding to 100 mCi of ^{131}I, and 5 mg kg^{-1} of DOX) for four times were sacrificed at 80 d p.i. Blood samples (≈0.8 mL) from mice were collected for blood biochemistry examination and complete blood panel. Meanwhile, major organs including liver, spleen, kidney, heart, lung were collected, fixed in 4% formalin, conducted with paraffin embedded sections, stained with H&E, and examined under a digital microscope (Olympus).

Supporting Information

Supporting Information is available from the Wiley Online Library or from the author.

Acknowledgements

This work was partially supported by the National Basic Research Program of China (973 Program 2014CB931900), National Natural Science Foundation of China (81471716, 81302383, 31400861, 21207164), the National Natural Science Foundation of Jiangsu Province (BK20140320), and a Project Funded by the Priority Academic Program Development of Jiangsu Higher Education Institutions (PAPD).

Received: August 25, 2015
Revised: September 15, 2015
Published online: November 5, 2015

[1] L. Fan, K. Strasser-Weippl, J. J. Li, J. St. Louis, D. M. Finkelstein, K. D. Yu, W. Q. Chen, Z. M. Shao, P. E. Goss, *Lancet Oncol.* **2014**, *15*, e279.
[2] D. Yoo, J. H. Lee, T. H. Shin, J. Cheon, *Acc. Chem. Res.* **2011**, *44*, 863.
[3] W. P. Tew, H. B. Muss, G. G. Kimmick, V. E. Von Gruenigen, S. M. Lichtman, *J. Clin. Oncol.* **2014**, *32*, 2553.
[4] P. McGale, C. Taylor, C. Correa, D. Cutter, F. Duane, M. Ewertz, R. Gray, G. Mannu, R. Peto, T. Whelan, Y. Wang, Z. Wang, S. Darby, *Lancet* **2014**, *383*, 2127.
[5] S. Darby, P. McGale, C. Correa, C. Taylor, R. Arriagada, M. Clarke, D. Cutter, C. Davies, M. Ewertz, J. Godwin, R. Gray, L. Pierce, T. Whelan, Y. Wang, R. Peto, *Lancet* **2011**, *378*, 1707.
[6] M. Clarke, R. Collins, S. Darby, C. Davies, P. Elphinstone, V. Evans, J. Godwin, R. Gray, C. Hicks, S. James, E. MacKinnon, P. McGale, T. McHugh, R. Peto, C. Taylor, Y. Wang, *Lancet* **2005**, *366*, 2087.
[7] J. E. Bekelman, G. Sylwestrzak, J. Barron, J. Liu, A. J. Epstein, G. Freedman, J. Malin, E. J. Emanuel, *JAMA, J. Am. Med. Assoc.* **2014**, *312*, 2542.
[8] T. A. Buchholz, E. A. Mittendorf, K. K. Hunt, *J. Natl. Cancer. Inst. Monogr.* **2015**, *2015*, 11.
[9] P. Pedrazzoli, M. Martino, S. Delfanti, D. Generali, G. Rosti, M. Bregni, F. Lanza, *J. Natl. Cancer. Inst. Monogr.* **2015**, *2015*, 70.
[10] L. Del Mastro, S. De Placido, P. Bruzzi, M. De Laurentiis, C. Boni, G. Cavazzini, A. Durando, A. Turletti, C. Nistico, E. Valle, O. Garrone, F. Puglisi, F. Montemurro, S. Barni, A. Ardizzoni, T. Gamucci, G. Colantuoni, M. Giuliano, A. Gravina, P. Papaldo, C. Bighin, G. Bisagni, V. Forestieri, F. Cognetti, *Lancet* **2015**, *385*, 1863.
[11] R. Peto, C. Davies, J. Godwin, R. Gray, H. C. Pan, M. Clarke, D. Cutter, S. Darby, P. McGale, C. Taylor, Y. C. Wang, J. Bergh, A. Di Leo, K. Albain, S. Swain, M. Piccart, K. Pritchard, *Lancet* **2012**, *379*, 432.
[12] Y. Tian, X. Jiang, X. Chen, Z. Shao, W. Yang, *Adv. Mater.* **2014**, *26*, 7393.
[13] Y. Min, C. Q. Mao, S. Chen, G. Ma, J. Wang, Y. Liu, *Angew. Chem. Int. Ed.* **2012**, *51*, 6742.
[14] A. R. Kirtane, S. M. Kalscheuer, J. Panyam, *Adv. Drug Delivery Rev.* **2013**, *65*, 1731.
[15] X. W. Ma, Y. L. Zhao, X. J. Liang, *Acta Pharmacol. Sin.* **2011**, *32*, 543.
[16] S. Mura, J. Nicolas, P. Couvreur, *Nat. Mater.* **2013**, *12*, 991.
[17] C. Sanson, C. Schatz, J. F. Le Meins, A. Soum, J. Thevenot, E. Garanger, S. Lecommandoux, *J. Control. Rel.* **2010**, *147*, 428.
[18] L. Wang, Q. Sun, X. Wang, T. Wen, J. J. Yin, P. Wang, R. Bai, X. Q. Zhang, L. H. Zhang, A. H. Lu, C. Chen, *J. Am. Chem. Soc.* **2015**, *137*, 1947.
[19] X. Yang, J. J. Grailer, I. J. Rowland, A. Javadi, S. A. Hurley, V. Z. Matson, D. A. Steeber, S. Gong, *ACS Nano* **2010**, *4*, 6805.
[20] Y. Saadeh, T. Leung, A. Vyas, L. S. Chaturvedi, O. Perumal, D. Vyas, *J. Nanosci. Nanotechnol.* **2014**, *14*, 913.
[21] L. Chen, X. Zhong, X. Yi, M. Huang, P. Ning, T. Liu, C. Ge, Z. Chai, Z. Liu, K. Yang, *Biomaterials* **2015**, *66*, 21.
[22] Z. Zhang, J. Wang, C. Chen, *Adv. Mater.* **2013**, *25*, 3869.
[23] J. Su, F. Chen, V. L. Cryns, P. B. Messersmith, *J. Am. Chem. Soc.* **2011**, *133*, 11850.
[24] H. Chen, G. D. Wang, Y. J. Chuang, Z. Zhen, X. Chen, P. Biddinger, Z. Hao, F. Liu, B. Shen, Z. Pan, J. Xie, *Nano Lett.* **2015**, *15*, 2249.
[25] Z. Zhen, W. Tang, C. Guo, H. Chen, X. Lin, G. Liu, B. Fei, X. Chen, B. Xu, J. Xie, *ACS Nano* **2013**, *7*, 6988.
[26] Z. Zhen, W. Tang, H. Chen, X. Lin, T. Todd, G. Wang, T. Cowger, X. Chen, J. Xie, *ACS Nano* **2013**, *7*, 4830.
[27] S. Mitragotri, D. G. Anderson, X. Chen, E. K. Chow, D. Ho, A. V. Kabanov, J. M. Karp, K. Kataoka, C. A. Mirkin, S. H. Petrosko, J. Shi, M. M. Stevens, S. Sun, S. Teoh, S. S. Venkatraman, Y. Xia, S. Wang, Z. Gu, C. Xu, *ACS Nano* **2015**, *9*, 6644.
[28] Z. Wang, Y. Wang, J. Zhao, J. S. Gutkind, A. Srivatsan, G. Zhang, H. S. Liao, X. Fu, A. Jin, X. Tong, G. Niu, X. Chen, *ACS Nano* **2015**, *9*, 6683.
[29] R. Chakravarty, H. F. Valdovinos, F. Chen, C. M. Lewis, P. A. Ellison, H. Luo, M. E. Meyerand, R. J. Nickles, W. Cai, *Adv. Mater.* **2014**, *26*, 5119.
[30] H. Hong, K. Yang, Y. Zhang, J. W. Engle, L. Feng, Y. Yang, T. R. Nayak, S. Goel, J. Bean, C. P. Theuer, T. E. Barnhart, Z. Liu, W. Cai, *ACS Nano* **2012**, *6*, 2361.
[31] X. R. Song, X. Wang, S. X. Yu, J. Cao, S. H. Li, J. Li, G. Liu, H. H. Yang, X. Chen, *Adv. Mater.* **2015**, *27*, 3285.
[32] J. Li, C. Zheng, S. Cansiz, C. Wu, J. Xu, C. Cui, Y. Liu, W. Hou, Y. Wang, L. Zhang, I. T. Teng, H. H. Yang, W. Tan, *J. Am. Chem. Soc.* **2015**, *137*, 1412.
[33] N. Lozano, W. T. Al-Jamal, A. Taruttis, N. Beziere, N. C. Burton, J. Van den Bossche, M. Mazza, E. Herzog, V. Ntziachristos, K. Kostarelos, *J. Am. Chem. Soc.* **2012**, *134*, 13256.
[34] X. Yi, K. Yang, C. Liang, X. Zhong, P. Ning, G. Song, D. Wang, C. Ge, C. Chen, Z. Chai, Z. Liu, *Adv. Funct. Mater.* **2015**, *25*, 4689.
[35] J. Park, T. F. Brust, H. J. Lee, S. C. Lee, V. J. Watts, Y. Yeo, *ACS Nano* **2014**, *8*, 3347.
[36] P. Zhang, J. Li, M. Ghazwani, W. Zhao, Y. Huang, X. Zhang, R. Venkataramanan, S. Li, *Biomaterials* **2015**, *67*, 104.
[37] Y. Liu, K. Ai, L. Lu, *Chem. Rev.* **2014**, *114*, 5057.
[38] L. S. Lin, Z. X. Cong, J. B. Cao, K. M. Ke, Q. L. Peng, J. Gao, H. H. Yang, G. Liu, X. Chen, *ACS Nano* **2014**, *8*, 3876.
[39] Y. Liu, K. Ai, J. Liu, M. Deng, Y. He, L. Lu, *Adv. Mater.* **2013**, *25*, 1353.

[40] Y. Xie, B. Yan, H. Xu, J. Chen, Q. Liu, Y. Deng, H. Zeng, *ACS Appl. Mater. Inter.* **2014**, *6*, 8845.
[41] X. Liu, J. Cao, H. Li, J. Li, Q. Jin, K. Ren, J. Ji, *ACS Nano* **2013**, *7*, 9384.
[42] C. K. Choi, J. Li, K. Wei, Y. J. Xu, L. W. Ho, M. Zhu, K. K. To, C. H. Choi, L. Bian, *J. Am. Chem. Soc.* **2015**, *137*, 7337.
[43] K. Y. Ju, Y. Lee, S. Lee, S. B. Park, J. K. Lee, *Biomacromolecules* **2011**, *12*, 625.
[44] H. Lee, S. M. Dellatore, W. M. Miller, P. B. Messersmith, *Science* **2007**, *318*, 426.
[45] H. Lee, J. Rho, P. B. Messersmith, *Adv. Mater.* **2009**, *21*, 431.
[46] Z. Liu, A. C. Fan, K. Rakhra, S. Sherlock, A. Goodwin, X. Chen, Q. Yang, D. W. Felsher, H. Dai, *Angew. Chem. Int. Ed.* **2009**, *48*, 7668.
[47] Z. Liu, X. Sun, N. Nakayama-Ratchford, H. Dai, *ACS Nano* **2007**, *1*, 50.
[48] Z. Liu, J. T. Robinson, X. Sun, H. Dai, *J. Am. Chem. Soc.* **2008**, *130*, 10876.
[49] Y. Tu, L. Zhu, *J. Controlled Release* **2015**, *212*, 94.
[50] Y. Sun, W. Zou, S. Bian, Y. Huang, Y. Tan, J. Liang, Y. Fan, X. Zhang, *Biomaterials* **2013**, *34*, 6818.
[51] K. T. Al-Jamal, W. T. Al-Jamal, J. T. Wang, N. Rubio, J. Buddle, D. Gathercole, M. Zloh, K. Kostarelos, *ACS Nano* **2013**, *7*, 1905.
[52] K. J. Chen, E. Y. Chaung, S. P. Wey, K. J. Lin, F. Cheng, C. C. Lin, H. L. Liu, H. W. Tseng, C. P. Liu, M. C. Wei, C. M. Liu, H. W. Sung, *ACS Nano* **2014**, *8*, 5105.
[53] K. J. Chen, H. F. Liang, H. L. Chen, Y. Wang, P. Y. Cheng, H. L. Liu, Y. Xia, H. W. Sung, *ACS Nano* **2013**, *7*, 438.
[54] C. Wang, H. Xu, C. Liang, Y. Liu, Z. Li, G. Yang, L. Cheng, Y. Li, Z. Liu, *ACS Nano* **2013**, *7*, 6782.
[55] Q. Fan, K. Cheng, X. Hu, X. Ma, R. Zhang, M. Yang, X. Lu, L. Xing, W. Huang, S. S. Gambhir, Z. Cheng, *J. Am. Chem. Soc.* **2014**, *136*, 15185.
[56] H. Ceylan, M. Urel, T. S. Erkal, A. B. Tekinay, A. Dana, M. O. Guler, *Adv Funct. Mater.* **2013**, *23*, 2081.